Engineering Structures 194 (2019) 36–45

Contents lists available at ScienceDirect

Engineering Structures

journal homepage: www.elsevier.com/locate/engstruct

Global sensitivity analysis of reliability of structural bridge system

Zdeněk Kala

Brno University of Technology, Faculty of Civil Engineering, Department of Structural Mechanics, Veveri Street 95, 602 00 Brno, Czech Republic

ARTICLE INFO

Keywords:
Sensitivity analysis
Fatigue
Bayesian probability
Steel bridge
Service life
Reliability

ABSTRACT

The article deals with the analysis of the probability of failure of a load-bearing steel bridge member under bending. The focus is on fatigue failure caused by stress cycles from multiple repeated traffic loading on the bridge. Failure is defined by the occurrence of a fatigue crack of critical size. Crack propagation and the fatigue limit state are described using linear fracture mechanics. The failure probability is a function of the equivalent stress range, initial crack length, Paris exponent, number of load cycles (stress changes) increasing over time and other input random variables. The failure probability is evaluated in time steps and then studied using a new type of global sensitivity analysis subordinated to contrasts. The results of the sensitivity analysis show that the first (second) dominant variable is the equivalent stress range (initial crack length) at any given point in time of the bridge operation. Strong main effect of equivalent stress range is associated with higher values of failure probability at the end of the lifetime of the bridge. Small values of failure probability are strongly influenced by interactions among input variables, which cannot be expressed as the sum of main effects of the individual input variables. The main and higher-order indices of each input variable are supplemented by displaying its total index. The direct goal of probability and sensitivity analysis is structural reliability. Sensitivity analysis confirms and deepens the knowledge gained from the time-dependent probability analysis. The numerical example illustrates the rationality of probability-oriented sensitivity indices and the feasibility of their estimation using Latin Hypercube Sampling (LHS). In addition, structural reliability is studied using Bayesian probability, which identifies the times for planning bridge inspections.

1. Introduction

Numerous bridges are approaching or have passed their expected service life. Fatigue is one of the more critical forms of damage that could potentially occur in steel bridges. Approximately 38% of collapses of steel bridges are due to fatigue [1]. Prediction and accurate assessment of the state of fatigue damage and the remaining fatigue life of steel bridges remains a challenging and unresolved task [2]. The assessment of an existing bridge with consideration to fatigue is typically performed using the same guidelines as for the design of new bridges [3]. However, these methods do not typically take into account large uncertainties on both the resistance side and the action effect side, which may have a significant effect on the reliability of the bridge.

Recently, a number of different methods for estimating the fatigue life of steel bridges have been proposed. Maljaars et al. [4] applied linear elastic fracture mechanics (LEFM) and FE modelling to the analysis of cracks growing into the deck plate from the root of the weld between the deck plate and stringer. Marques et al. [5] presented fatigue probabilistic analyses of steel riveted bridges based on LEFM and FE modelling of critical connections. In this context, sensitivity analysis (SA) was performed to obtain conclusions on the correlation between the fatigue life and the number of trains in each loading block [5]. Sun [6] developed a corrosion fatigue model describing the damage process due to the combined action of stress and corrosion of high-strength steel bridge cable wires. Peng [7] revealed the importance of the interaction between fatigue crack growth and the stress increase created by corrosion due to the reduction in the section thickness.

McAllistera and Ellingwood [8] have shown that stochastic fatigue analysis can be used to assess the fatigue performance observed in some miter gates and for the planning of inspections and maintenance. Tomica et al. [9,10], Krejsa et al. [11,12], Maljaars and Vrouwenvelder [13] and Leander et al. [3] evaluated the reliability and durability of steel bridges using LEFM and Bayesian probability, which is used as the basis for proposing a system of inspections of the construction. It may be noted that similar approaches are used to plan reliability-based inspections of structural details of ships [14]. However, modern reliability analyses must go much further than to estimate the optimal bridge inspection times based on probability analysis.

The aforementioned probabilistic assessments of reliability are generally not SA-oriented in order to evaluate how the input random variables and their interactions influence the output failure probability. Then, researchers cannot decide how to devote data collection

E-mail address: kala.z@fce.vutbr.cz.

https://doi.org/10.1016/j.engstruct.2019.05.045
Received 12 November 2018; Received in revised form 2 May 2019; Accepted 16 May 2019

resources so as to most effectively reduce uncertainty of model output [15]. Global sensitivity analysis (GSA), which is capable of identifying the most critical and essential contributors to output uncertainty and risk, is one of such techniques in solving this problem [16]. Using the GSA results researchers can pay increased attention to the more important input variables to provide increased control of the probability of failure of the structure and simplify the model by fixing the less important input variables at their nominal values without significantly influencing the probability of failure of the structure [17].

In the last several decades, various approaches to compute SA have been proposed; see state-of-the-art reviews [18–20]. Commonly established SA methods can be summarized as non-parametric techniques [21], screening approaches [22], Sobol variance-based methods [23,24] and moment-independent methods [25], etc. Amongst these methods, Sobol's indices have received considerable attention because they not only quantify the relative importance of each variable, but also reflect the structure of the model response function [26]. Borgonovo [27] showed that variance is not always sufficient to describe uncertainty and indicated that a sensitivity measure should refer to the entire output distribution and not just to a particular moment.

The GSA methods mentioned above mainly focus on computational models with real-valued output and cannot be directly used in probability analysis of reliability. According to the conventional definition, the reliability SA investigates the rate of change in the failure probability due to the probability characteristics of a basic random variable [28]. One approach to SA is local SA (LSA), which measures sensitivity as the partial derivative of the failure probability (or reliability index) with respect to the distribution parameters of the input random variable [28–33]. The disadvantage of LSA is that it only provides information on sensitivity at the nominal point, where the derivative (sensitivity factor) is calculated, but cannot identify the interactions between different variables. GSA overcomes this deficiency because it measures the influence of input variables over their entire variation domains on structural failure probability including the quantification of the influence of interactions between input variables [17,25,34,35]. GSA is not limited by the form of the limit state function and the probability density functions (pdfs) of the inputs, but typically requires a large number of limit state function evaluations for favourable accuracy of calculation, see for e.g. [36–38]. Therefore, it is necessary to develop more efficient methods for the estimation of GSA with fewer calls to the time-consuming limit state function [25,39–41].

A fairly new type of GSA subordinated to contrast functions was presented in [42]. Fort et al. [42] denote contrast-based GSA as Goal Oriented Sensitivity Analysis (GOSA), because SA is oriented to parameters (goals) of the probability distribution model output, such as the mean value, quantile or probability. The selection of the contrast function can be used to determine global sensitivity indices of different types. It has been shown in [42] that use of the quadratic contrast function, which measures the average squared deviation from the mean, leads to the established Sobol sensitivity indices [23,24]. From the perspective of GOSA, Sobol GSA is oriented to the mean value as the central parameter. SSA is a subset of GOSA. Similarly, it is possible to select other classical contrasts associated with quantile [43–45]. GOSA includes both moment dependent (e.g. Sobol SA) moment independent (e.g. probability) methods and therefore has a more general classification. Numerical tests using the Ishigami function have shown that GOSA oriented to the median agree with Sobol GSA in the case of non-influential parameters with very small or zero values of sensitivity indices, otherwise the results are more or less different [44].

The basis of this article is the probability and sensitivity analysis of the reliability of a load-bearing steel bridge girder. Using Bayesian probability, the results of the probabilistic analysis are updated with regard to the results of bridge inspections that investigate the occurrence of fatigue cracks. New findings on the fatigue limit state are obtained mainly through the application of Contrast based SA [42], referred to as PSA in this article. PSA evaluates the influence of five input random variables (main effects, two-way interactions and all higher-order interactions) on the failure probability of a steel girder over time. The article presents a comprehensive concept of time-dependent probability and global sensitivity analysis of the reliability of steel girders with cracks.

2. Sensitivity analysis subordinated to contrasts

Reliability of building structures is generally a random variable, which is a function of random variables.

$$Z = g(X) = g(X_1, X_2, ...,X_M) \tag{1}$$

where Z is a scalar output and X_i are M statistically independent input variables. These variables generally represent geometric and material characteristics, load and other effects [46]. Failure occurs if $Z < 0$. The contrast function ψ associated with probability of failure $P_f = P(Z < 0)$ can be written using parameter θ as

$$\psi(\theta) = E(\psi(Z, \theta)) = E(1_{Z<0} - \theta)^2 \tag{2}$$

The probability estimator θ^* is defined by the equation $\theta^* = \text{Argmin}\ \psi(\theta)$. The first order probability contrast index C_i (main or first order sensitivity index subordinated to the contrast) can be expressed, on the basis of [42], as

$$C_i = \frac{\min_\theta \psi(\theta) - E(\min_\theta E(\psi(Z, \theta)|X_i))}{\min_\theta \psi(\theta)} \tag{3}$$

where the numerator is the contrast variation due to X_i. C_i is the sensitivity index of the estimator of θ^*. The minimum value of contrast $\psi(\theta)$ can be calculated, for e.g., using K runs of the Monte Carlo (MC) method as

$$\min_\theta \psi(\theta) \approx \frac{1}{K}\sum_{k=1}^{K}(1_{Z<0} - \theta^*)^2 \tag{4}$$

The failure probability θ^* can be estimated from MC runs so that $\theta^* \cdot K$ runs (failures) of Z are smaller than zero and $(1 - \theta^*)\cdot K$ runs of Z are greater than zero.

The second member in the numerator in Eq. (3) can be calculated using double-nested-loop simulation of the MC method. L random realizations of X_i, i.e. $X_i(1)$, …, $X_i(j)$,…, $X_i(L)$ are generated in the first set. Then, K random realizations of vector $X_{\sim i}$ are generated for each realization $X_i(j)$, $j = 1,…, L$ (all variables but X_i). For fixed X_i, it can be written that

$$\min_\theta E(\psi(Z, \theta)|X_i) \approx m_i(j) = \frac{1}{K}\sum_{k=1}^{K}(1_{g(X_i(j),X_{\sim}(j,k))\leq 0} - \theta_i^*(j))^2 \tag{5}$$

where conditional failure probability $\theta_i^*(j)$ is calculated as in Eq. (4), but the runs of Z are obtained for K random realizations of variables $X_{\sim i}$ and fixed X_i. For L runs of X_i we subsequently obtain

$$E(\min_\theta E(\psi(Z, \theta)|X_i)) = \frac{1}{L}\sum_{j=1}^{L} m_i(j) \tag{6}$$

The second-order probability contrast index C_{ij} measures the second-order interaction between X_i and X_j. C_{ij} is defined as

$$C_{ij} = \frac{\min_\theta \psi(\theta) - E(\min_\theta E(\psi(Z, \theta)|X_i, X_j))}{\min_\theta \psi(\theta)} - C_i - C_j \tag{7}$$

The higher-order probability contrast indices can be expressed analogously. The higher-order terms enable quantification of higher-order interactions by the analyst. Interactions represent important features of models and are more difficult to detect than the first order effects. The sum of all sensitivity indices must be equal to one.

$$\sum_i C_i + \sum_i \sum_{j>i} C_{ij} + \sum_i \sum_{j>i} \sum_{k>j} C_{ijk} + ... + C_{123...M} = 1 \tag{8}$$

It can be noted that the use of the contrast function $\psi(\theta) = E(Z - \theta)^2$ transforms Eqs. (3), (7) and Eq. (8) to the classical Sobol decomposition [23,24], in which the first order sensitivity index S_i is defined as

$$S_i = \frac{V(Z) - E(V(Z\,|X_i))}{V(Z)} = \frac{V(E(Z\,|X_i))}{V(Z)} = corr^2(Z, E(Z\,|X_i)) \tag{9}$$

where *corr* is Pearson correlation coefficient. Sobol higher-order sensitivity indices are calculated analogously, see e.g. [15]. It can be noted that other measures of corr, for e.g. Spearman's rank correlation or Kendall's τ also lead to the decomposition, where the sum of all indices is one. However, indices based on different correlation measurements differ slightly.

C_i, C_{ij}, and higher-order indices identify the significance of each variable in determining the output contrast of failure probability P_f. However, in the case of large numbers of input variables it would require the evaluation of 2^M-1 indices, which can be computationally demanding. Therefore, it may be more suitable to identify the influence of each variable using the total index C_{Ti}.

$$C_{Ti} = 1 - \frac{\min_{\theta} \psi(\theta) - E(\min_{\theta} E(\psi(Z, \theta)|X_{\sim i}))}{\min_{\theta} \psi(\theta)} \tag{10}$$

The total index C_{Ti} measures the contribution to the output contrast of X_i, including all contrast caused by its interactions, of any order, with any other input variables. The total index C_{Ti} can also be calculated with knowledge of C_i, C_{ij}, and higher-order indices if all sensitivity indices in Eq. (8) are calculated. For example, for $M = 3$ we can write $C_{T1} = C_1 + C_{12} + C_{13} + C_{123}$.

3. Fatigue crack propagation

3.1. Linear fracture mechanics

Paris-Erdogan law relates the stress intensity factor range to subcritical crack growth under a fatigue stress regime [47]. Fatigue crack growth can be analysed using the basic formula:

$$\frac{da}{dN} = D \cdot (\Delta K)^m \tag{11}$$

where a is the crack length, da/dN is the crack length growth per increasing number of load cycles, D and m are Paris constant and exponent. The stress rate coefficient ΔK is given as [48]

$$\Delta K = K_{\max} - K_{\min} = F(a) \cdot \Delta\sigma \cdot \sqrt{\pi \cdot a} \tag{12}$$

where $\Delta\sigma$ is the range of cyclic stress amplitude. $F(a)$ is the calibration function, which represents the course of propagation of the crack. $F(a)$ for pure bending was derived from experimental and numerical research [49,50,51] of fatigue cracks propagating from the edge as

$$F\left(\frac{a}{W}\right) = 1.114 - 0.8975\left(\frac{a}{W}\right) + 2.752\left(\frac{a}{W}\right)^2 + 1.1323\left(\frac{a}{W}\right)^3 \tag{13}$$

for relative crack length $a/W \in \langle 0.01,\ 0.5\rangle$, where W is the specimen width. Eq. (13) is for rectangular cross-sections under pure bending (member-specific) and may not be usable for other cases. The calibration curves for additional geometries can be found in handbooks [52,53]. For examples on the use of Eq. (13) see [54]. By modifying and integrating Eq. (11), it is possible to express the crack growth from length a_1 to a_2 and the corresponding increase in the number of cycles from N_1 to N_2:

$$\int_{a_1}^{a_2} \frac{da}{[F(a) \cdot \sqrt{\pi \cdot a}\,]^m} = \int_{N_1}^{N_2} D \cdot (\Delta\sigma)^m dN \tag{14}$$

The left side of Eq. (14) represents the accumulation of damage. A prerequisite for the stable propagation of the fatigue crack is the existence of the initiation crack a_0 at the point of stress concentration, which may be located on the edge or on the surface of the girder. Maximum fatigue damage occurs when the crack propagates from the initial length a_0 to the critical length a_{cr}, then brittle fracture occurs. The accumulation of damage for crack propagation from a_0 to a_{cr} can be introduced as the resistance of the structure $R(a_{cr})$.

$$R(a_{cr}) = \int_{a_0}^{a_{cr}} \frac{da}{[F(a) \cdot \sqrt{\pi \cdot a}\,]^m} \tag{15}$$

The value of $R(a_{cr})$ depends mainly on a_0 and much less on a_{cr}. Therefore, a_{cr} can be introduced with consideration to Eq. (13) as $a_{cr} = 0.5\,W$, see e.g. [55]. With regard to Eq. (13) and parameter m, the integration in Eq. (15) must be evaluated numerically. Simpson's rule with a smaller step near a_0 was used for the integration.

The right side of Eq. (14) represents the cumulative effects of the load. For bridge structures, it is justified to assume that the number of cycles at the time of initiation of the fatigue crack a_0 (initial cracks from drilling, cutting, etc.) is zero. Then the cumulated effects of the load can be expressed as:

$$S(t) = \int_0^N D \cdot (\Delta\sigma)^m dN = D \cdot N \cdot (\Delta\sigma)^m \tag{16}$$

where N is the total number of oscillations (number of load cycles at time t) of stress range $\Delta\sigma$ during crack propagation from a_0 to a_{cr}. Brittle fracture is the only failure type considered in this article. The reliability function can be written on the basis of Eq. (15) and Eq. (16) as:

$$Z = R(a_{cr}) - S(t) \tag{17}$$

3.2. Failure probability analysis

Eq. (17) is a function of the following random variables: mechanical properties (D, m), geometry (W), traffic load effects ($\Delta\sigma$, N) and dimensions of the initial (a_0) and critical (a_{cr}) fatigue crack. Paris constant D can be expressed as function m from the equation $\log(D) = d_1 + d_2 \cdot m$ where $d_1 = -11.141$ and $d_2 = -0.507$ [56]. The probability analysis of Eq. (17) gives the failure probability P_f:

$$P_f = P(F) = P(Z \leqslant 0) = P(R(a_{cr}) - S(t) \leqslant 0) \tag{18}$$

Eq. (18) expresses the probability of phenomenon F, when the crack has reached length a_{cr}. Probability P_f increases with the increasing number of cycles over time. The probabilistic approach not only makes it possible to evaluate P_f as a function of random parameters a_0, a_{cr}, m, $\Delta\sigma$, N, W, but in addition, the value of P_f can be updated by calculating the conditional probability using new information from regular inspections of bridges in operation.

Typical new information is the detection or nondetection of fatigue cracks during bridge inspection. Let us assume that propagation of the fatigue crack from the surface of the steel bridge girder is crucial for the service life of the bridge. Appropriate precautions should be taken if a crack of measurable length a_d is detected during inspection, for e.g. limit the crack growth, monitor crack propagation, suspend or restrict traffic on the bridge. In terms of use of the conditional probability, the second case (phenomenon I), when a crack is not detected, is interesting. This means that at a given location the crack has either not yet formed or has not reached a detectable size a_d. The probability of phenomenon I is

$$P_I = P(I) = P(R(a_d) - S(t) \geqslant 0) \tag{19}$$

where $R(a_{cd})$ is calculated from Eq. (15) for interval of integration $[a_0, a_d]$. In subsequent years of operation, the probability of failure can be calculated using the conditional probability P_{fI}.

$$P_{fI} = P(F\,|I) = \frac{P(F \cap I)}{P(I)} \tag{20}$$

Table 1
Input random variables.

No	Symbol	Characteristic	Density	Mean μ	Standard deviation σ
1	$\Delta\sigma$	Equivalent stress range	Gauss	30 MPa	3 MPa
2	a_0	Initial edge crack length	log-normal	0.2 mm	0.06 mm
3	m	Paris exponent	Gauss	3	0.03
4	N_y	Number of load cycles per one hundredth of a year	Gauss	1E4	1E4
5	W	Specimen width	Gauss	400 mm	20 mm
6	a_d	Smallest detectable crack length	Gauss	10 mm	0.6 mm

P_{fI} represents the probability of failure (the crack reaches a_{cr} - phenomenon F), provided that failure was not observed during prior inspection (phenomenon I). $P(F \cap I)$ represents the intersection of phenomena F and I.

4. Probabilistic calculation

4.1. Input random variables

The initial length a_0 of the edge crack is considered using a log-normal pdf with mean value of 0.2 mm and standard deviation of 0.06 mm [57,12,54], see Table 1. These values were considered for basic (standard) structural steel grade S235 and cannot represent general cases. In general, the initial crack length is dependent on the method of its measurement (x-ray, kapilar, etc.) and material type. Log-normal pdf of a_0 is a suitable type of probability distribution, which was also confirmed by the inverse analysis of the fatigue resistance [58]. It can be noted that the standard deviation is up to ten times lower in comparison with the initial crack of an as-welded detail [3,4].

In practice, bridges are exposed to a complex, random sequence of loads, large and small. In order to assess the safe remaining life of such structures the complex loads can be reduced to simple equivalent cyclic load, which results in the same fatigue damage as the original loading spectrum. The equivalent stress range Δσ is the range of cyclic stress amplitude (form the equivalent cyclic load), which replaces the actual histogram of stress range (from the actual load) [59].

The uncertainty of $\Delta\sigma$ is associated with the uncertainty of the spectrum of the stress range, which contributes to the overall fatigue damage [59]. The mean value and standard deviation of $\Delta\sigma$ can be computed using the actual histogram of stress range from long-term monitoring program. The stress range histogram data are obtained by rain-flow counting method from the monitoring data [60]. All small cycles that do not contribute to the overall fatigue damage are neglected. The histogram of stress range is truncated by the predefined cut-off stress range and then approximated by appropriate pdfs (Log-normal, Weibull, Gamma etc.) [59]. The mean value and standard deviation of $\Delta\sigma$ are associated with uncertainties in the assumed pdf and cut-off of stress range.

Gauss pdf and statistical characteristics of Δσ are introduced acc. to [11,12]. The statistical model of Δσ in Table 1 assumes that the axle weights in each time interval occur with the same frequency, but there is uncertainty in their magnitudes. Gauss pdf of the other input random variables listed in Table 1 are considered acc. to: m [54,55,58], W [46,54,58] and a_d [11,12].

The number of load cycles (stress changes) [11,12,54] per year is transformed for the time step of a hundredth of a year. With the exception of N_y and a_0, the Gauss pdfs in Table 1 are truncated in the interval $[\mu - 6{\cdot}\sigma, \mu + 6{\cdot}\sigma]$ so that negative values of the random realizations of MC are not obtained. Log-normal pdf of a_0 is truncated in the interval [0, 6]. It can be noted that the probability of the occurrence of MC samples of untruncated variables in Table 1 outside the truncation intervals is practically negligible.

4.2. Monte Carlo simulations

The calculation of P_f in Eq. (18) is performed using the MC method with the time step of one hundredth of a year. The estimate of P_f is calculated using n simulation runs in time t. The same set of (pseudo-) random numbers is used in each time step (for each estimate of P_f), thereby ensuring that sampling and numerical errors do not swamp the result being sought [30,61]. The number of load cycles N_t (stress changes) in time t is calculated as the sum N_y.

$$N_t = \sum_{y=1}^{t} N_y \tag{21}$$

where N_y is the number of loading cycles (stress changes) per one hundredth of a year and $t = 1, 2\ldots12{,}000$ is the number of hundredths of years of operation of the bridge. After all values of N_t are calculated the sequence of random realizations of N_t is adjusted to be non-decreasing. The algorithm can be clearly written in the programming language Pascal as: for $t:=1$ to 11,999 do if $N_{t+1} < N_t$ then $N_{t+1} := N_t$. For the time step of a hundredth of a year, $N_{t+1} < N_t$ occurs in approximately 16% of the samples. It can be noted that the frequency of observations $N_{t+1} < N_t$ decreases very rapidly for the time step greater than one tenth of the year. Conversely, a time step, which is smaller than a hundredth of a year, does not significantly increase the accuracy numerically.

Once the target failure probability $P_f \to P_{ft}$ is reached at time t_1, an inspection is performed and n_1 observations $R(a_d) \leqslant S(t)$, where the crack is detected, are eliminated from the random sample. The calculation of the conditional probability P_{fI} Eq. (20) of Path 1 is performed using the remaining n-n_1 MC runs for which no crack was detected during the first inspection. Once $P_f \to P_{ft}$ at time t_2 a second inspection is performed and additional n_2 observations $R(a_d) \leqslant S(t)$ are eliminated from the random sample. The calculation of P_{fI} of Path 2 is performed using the remaining n-n_1-n_2 MC simulation runs for which no crack was detected during the previous two inspections. The procedure is repeated for the calculation of the other branches P_{fI}. The accuracy of the probabilistic calculation of the other branches P_{fI} gradually decreases with increasing number of inspections because the probability is calculated from an even smaller number of simulation runs. For this reason, the calculation of P_f (Path 0) must be started with a sufficiently large number of MC simulation runs.

An illustrative example of the calculation of P_{fI} using the MC method is shown in Fig. 1. For $n = 10$ we can write $P_{fI} = P(F\,|I) = P(F \cap I)/P(I) = 2/7$.

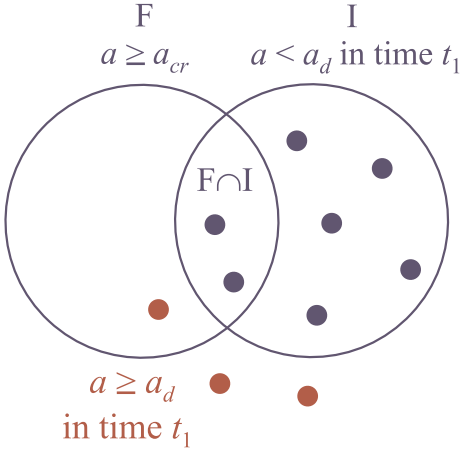

Fig. 1. Example of the calculation of P_{fI} based on 10 specific simulations.

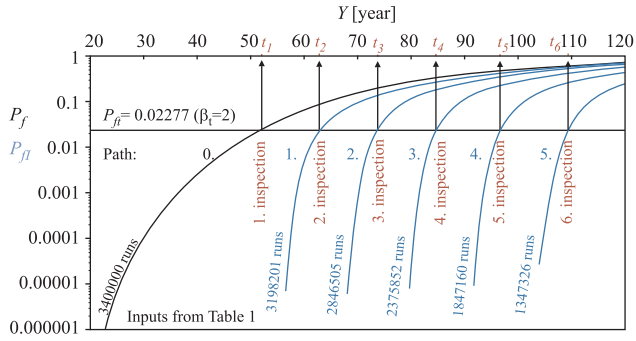

Fig. 2. Failure probability P_f vs. time.

4.3. Failure probability analysis

For service life of 50 years, standard ISO 13822 [62] proposes target reliability indices of $\beta_t = 3.1$ and $\beta_t = 2.3$ for non-inspectable and inspectable details, respectively. The first inspection should be scheduled before the end of the planned service life of the bridge. Therefore, the target reliability index value is chosen to be lower than 2.3 as $\beta_t = 2$, which corresponded to the target failure probability $P_{ft} = 0.02277$.

Path 0: The failure probability P_f Eq. (18) is analysed in dependence on the time of bridge operation, which is shown for clarity with the unit of one year, see Fig. 2. The MC method is used to generate $n = 3.4$ million random sampling of 12,005 input random variables in Table 1. The estimate of P_f is calculated with a time step of a hundredth of a year using Eq. (21). For example, for $t = 2$, input random variables $\Delta\sigma$, a_0, m, N_1, N_2, W are used to estimate P_f. P_f (Path 0) is plotted on a logarithmic scale as a polygon (line segments from point to point) calculated from 12,000 points of P_f and plotted for $P_f > 1E-6$, see Fig. 2. Polygon Path 0 shown in Fig. 2 appears to be a smooth curve. This is due to the high number of MC runs and calculation method of P_f, in which the same set of (pseudo-) random numbers is used for $\Delta\sigma$, a_0, m, N_y, W in each time step, and where the growth of P_f is due to the increasing value of N_t acc. to Eq. (21). The same applies for the other paths. Identical paths as in Fig. 2 can be obtained using a different set of (pseudo-) random numbers, very small numerical differences are negligible from a technical point of view.

Path 1: n_1 observation $a > a_d$ is excluded from n runs at time t_1, in which $P_f \approx P_{ft}$. The conditional probability P_{fl} Eq. (20) plotted as Path 1 is calculated using n-n_1 = 3,198,201 runs of MC, see Fig. 2. The process of excluding n_1 random realizations of input variables $\Delta\sigma$, a_0, m is shown in Figs. 3–5 in red, unexcluded n-n_1 observations are blue. Particularly in the case of random variables $\Delta\sigma$ and a_0 it is observed

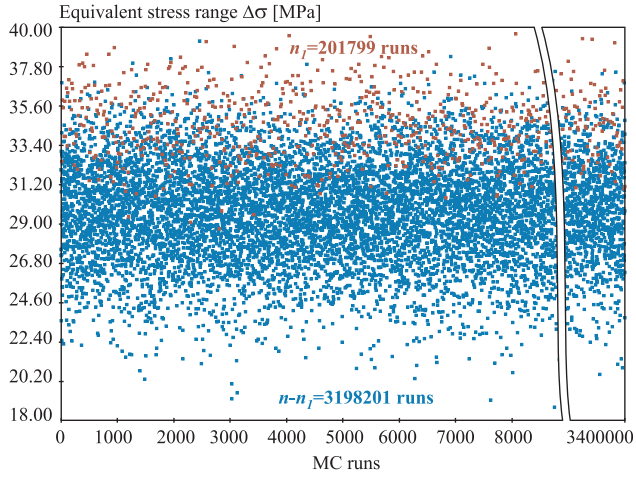

Fig. 3. Separation of random samples $\Delta\sigma$ in time t_1.

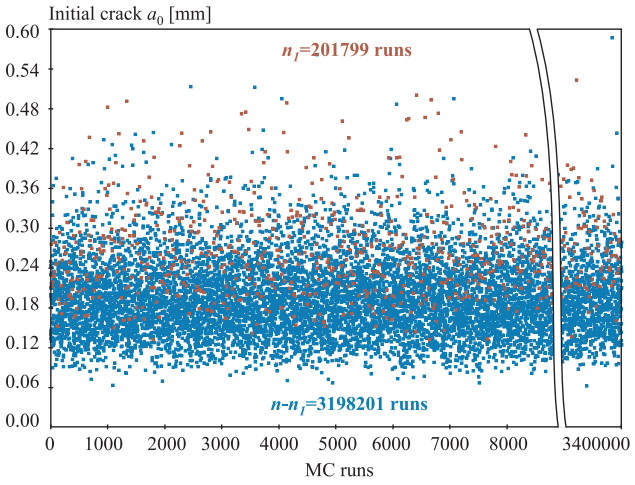

Fig. 4. Separation of random samples a_0 in time t_1.

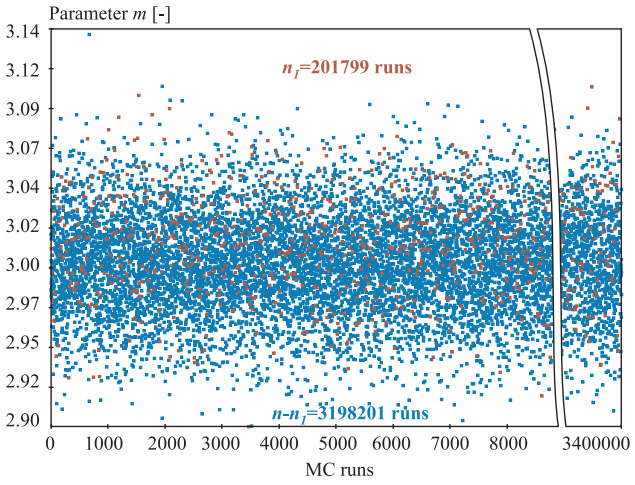

Fig. 5. Separation of random samples m in time t_1.

that predominantly higher values of random realizations of $\Delta\sigma$ and a_0 are excluded. On the contrary, the spectrum of excluded and unexcluded observations of parameter m (see Fig. 5) and other variables W, N_t is approximately the same.

The process of excluding further observations n_2, n_3, n_4, n_5 (on level P_{ft} at time t_2, t_3, t_4, t_5) is similar. It can be noted that the initial $n = 3.4$ million runs of the MC method are reduced to 1,347,326 after five inspections, see Path 5 on Fig. 2. This means that the detected crack is not found during the first five inspections with approximately 40% probability 1.347/3.4 ≈ 0.4. Path 5 is calculated with 1,347,326 values of random realizations of $\Delta\sigma$, a_0, m, N_t, W, which during previous inspections fulfilled the condition $a < a_d$.

Input random variables in Table 1 are considered as statistically independent. However, this does not apply to the gradual exclusion of n_1, n_2, n_3, n_4, n_5 from n observations. The gradual exclusion introduces correlation between some input variables, see Table 2. In Table 2, the notation corr($\Delta\sigma$, a_0) defines Pearson correlation between $\Delta\sigma$ and a_0, corr($\Delta\sigma$, m) is Pearson correlation between $\Delta\sigma$ and m, corr(a_0, m) is Pearson correlation between a_0 and m. Corr($\Delta\sigma$, a_0) results from the reduction of samples in time t_1, see Fig. 6. Correlations between the other variables are less significant. Correlation between samples has an underlying effect on the plots of P_{fl}. Correlation with $\Delta\sigma$ has the primary effect of extending the inspection intervals.

Table 2
Pearson correlation between input variables.

Path	Runs	corr($\Delta\sigma$, a_0)	corr($\Delta\sigma$, m)	corr(a_0, m)
0	n = 3,400,000	≈0	≈0	≈0
1	n-n_1 = 3,198,201	−0.106	−0.053	−0.032
2	n-n_1-n_2 = 2,846,505	−0.199	−0.097	−0.053
3	n-n_1-n_2-n_3 = 2,375,852	−0.284	−0.134	−0.067
4	n-n_1-n_2-n_3-n_4 = 1,847,160	−0.360	−0.170	−0.072
5	n-n_1-n_2-n_3-n_4-n_5 = 1,347,326	−0.426	−0.197	−0.074

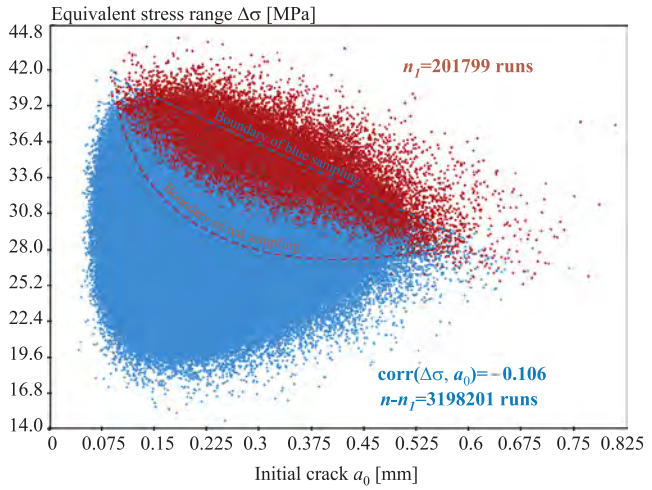

Fig. 6. Separation of random samples a_0 vs. $\Delta\sigma$ in time t_1.

4.4. Failure probability results

Inspections and maintenances can be planned at times t_1, t_2, t_3, etc. when Path 0, 1, 2, etc. intersect level P_{ft}, see Fig. 2. Inspection intervals are an important output of the probabilistic analysis, see Fig. 2. The first three inspection intervals are approximately constant, the other two are slightly longer: $(t_2\text{-}t_1) \approx (t_3\text{-}t_2) \approx (t_4\text{-}t_3) < (t_5\text{-}t_4) < (t_6\text{-}t_5)$, see Fig. 2.

It can be noted that the theoretical introduction of $\Delta\sigma$ as a deterministic (non-random) value leads to perfect periodic and also later inspection intervals, see Fig. 7. However, due to loading uncertainties, a probabilistic approach considering uncertainty of equivalent stress range $\Delta\sigma$ is used.

In the statistical model in Table 1, any change in the mean value or standard deviation of $\Delta\sigma$ has a significant influence on P_f and changes all paths shown in Fig. 2. For example, increasing the mean value of $\Delta\sigma$ from 30 MPa to 31 MPa with the same variation coefficient of 0.1 leads to inspections in 46.9, 56.8, 66.6, 76.8, 87.7, 99.5 years, which is an approximately 90 percent reduction in inspection times compared to Fig. 2. Inspection in 9.2, 11.2, 13.2, 15.2, 17.3 etc. years (approximately every two years) would theoretically be obtained by using the

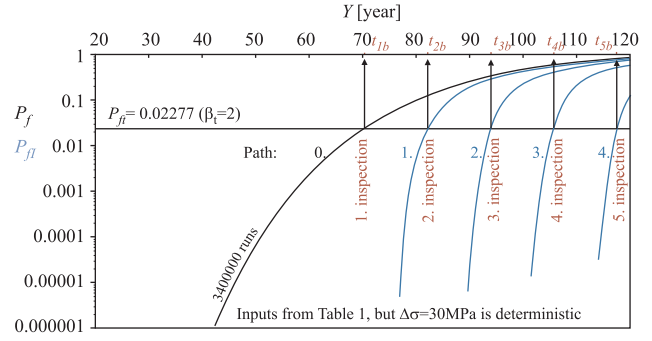

Fig. 7. Failure probability P_f vs. time, $\Delta\sigma$ is deterministic.

mean value of $\Delta\sigma$ of 53 MPa with variation coefficient 0.1. The introduction of a higher variation coefficient of $\Delta\sigma$ leads to earlier and prolonged (non-periodic) inspection intervals [54].

The probabilistic analysis results shown in Fig. 2 may also be discussed in connection with the intensity of degradation processes that may contribute to the growth of fatigue cracks, see e.g. [7,63]. Deterioration of the resistance to fatigue crack propagation in dependence on the intensity of the degradation processes may increase the probability of failure, especially at the end phase of the service life of the bridge. On the other hand, degradation processes can be partially eliminated by regular maintenance, for e.g. at times of bridge inspection.

5. Sensitivity analysis results

5.1. Estimation of sensitivity indices

PSA is evaluated for unconditional probability of failure P_f, see Path 0 (black line) in Fig. 2. The influence of five random variables $\Delta\sigma$, a_0, m, N, W on P_f is analysed. PSA evaluated the contribution of each input to the uncertainty of P_f. In order to calculate PSA, the equation with the sum Eq. (21) is substituted with one random variable N with mean value $\mu_N = Y{\cdot}1E6$ and standard deviation $\sigma_N = \sqrt{Y}{\cdot}1E5$ [54], where Y is the number of years of operation of the bridge. Gauss pdf of N is truncated to the interval $[\mu_N - 6{\cdot}\sigma_N, \mu_N + 6{\cdot}\sigma_N]$.

Sensitivity indices Eq. (8) are estimated using relatively high number of runs of the Latin Hypercube Sampling method [64,65]. It can be noted that in simulations with double-nested-loop the LHS method does not lose its advantages over the MC method even in applications with very high numbers of simulation runs. For example, for Y = 35 years, each sensitivity index in Eq. (8) is estimated using K = 87E6, L = 2E4 of LHS runs. For Y = 35 years, a very high number of simulation runs K = 87E6 is needed to evaluate small probabilities of failure in the nested-loop of PSA, see for e.g. Eq. (5). In times Y > 35 years, a smaller number of LHS runs is applied acc. to the equation $K = 5E4/P_f$, but $K \geqslant 6E6$, where P_f is the full line in Fig. 2. The outer loop uses L = 2E4 for each Y, see for e.g. Eq. (6).

PSA is evaluated using a time step of 5 years. All $2^5-1 = 31$ sensitivity indices in Eq. (8) are estimated at each time step. Each sensitivity index is calculated at each time step as the arithmetic mean of its 16 estimates (computed on 16 CPU cores), where each estimate uses a different set of (pseudo-) random numbers. By doing so, the sum of all indices in decomposition Eq. (8) is equal to one with an accuracy greater than 1E−4.

All 31 sensitivity indices for three selected times Y = 35, 60, 120 years are shown in Figs. 8–10. PSA performs the task of ordering by importance the strength and relevance of the inputs in determining the uncertainty of the P_f. The numerical results indicate that $\Delta\sigma$ is the most dominant variable in all cases.

Fig. 10 (Fig. 9) shows that $\Delta\sigma$ has a very strong 54% (36%) main effect on P_f. In LHS simulations, fixing small (large) values of $\Delta\sigma$ significantly decreases (increases) P_f. Decreasing the value of $\Delta\sigma$ significantly reduces P_f and increases the reliability and residual life of aging bridges. Practically, this can be achieved by prohibiting the passage of very heavy vehicles, which can extend the lifespan of the bridge at the end of the lifetime, when repairs of fatigue failure cannot provide sufficient reliability or are uneconomical.

Fig. 10 (Fig. 9) shows moderate interaction effects of 11% (20%) of the pair $\Delta\sigma$, a_0 on P_f. In LHS simulations, interactions occur when the perturbation of two or more inputs simultaneously causes changes in the P_f greater than that of varying each of the inputs alone. Fatigue failures are caused mainly by random realizations of pairs with higher value of $\Delta\sigma$ and higher value of a_0. The reliability of the bridge can be effectively increased by reducing the magnitude of $\Delta\sigma$ and repairing bridges with developed cracks $a > a_d$, which are identified during regular inspections, see e.g. Fig. 6. For middle-aged bridges, it is not

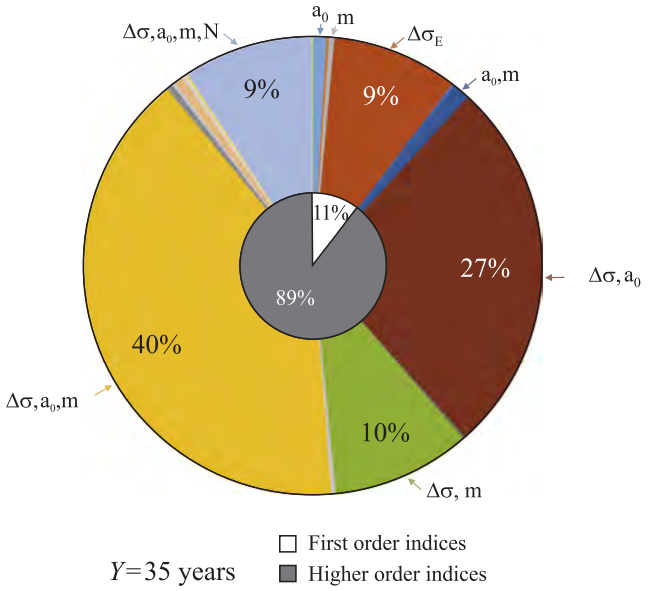

Fig. 8. First and higher-order sensitivity indices, Y = 35 years.

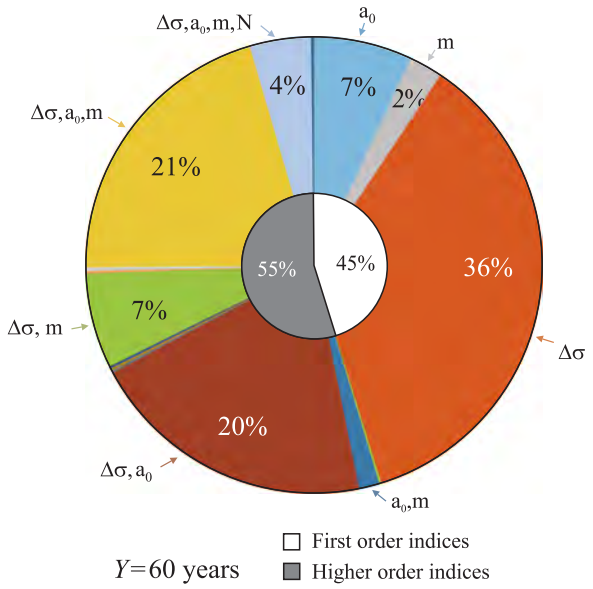

Fig. 9. First and higher-order sensitivity indices, Y = 60 years.

effective to prohibit the passage of heavy vehicles in order to extend the bridge lifetime if the bridges can be inspected and repaired.

Fig. 8 shows that the main effect of $\Delta\sigma$ is 9% and that strong interaction effects with $\Delta\sigma$ are present. The second-order interaction effect of $\Delta\sigma$, a_0 is 27%, second-order interaction effect of $\Delta\sigma$, m is 10%, third-order interaction effect of $\Delta\sigma$, a_0, m is 40%, fourth-order interaction effect of $\Delta\sigma$, a_0, m, N is 9%. The main effect of a_0 is minimal, however, interactions of a_0 with $\Delta\sigma$ and other variables are relatively significant. Overall, interactions reach 89%. In 35 years of bridge operation, traffic-related fatigue failure are not very probable ($P_f \approx 6E-4$) and occur particularly as a result of unfavourable combinations of $\Delta\sigma$, a_0 or $\Delta\sigma$, a_0, m.

Inspections focused on fatigue failure caused by traffic can be planned after the target failure probability P_{ft} = 0.02277 is reached, see Fig. 2. It can be noted that the presented case study analyses the occurrence of fatigue failure only from traffic load and does not consider other negative influences that may hasten the need for inspections.

Trends of crucial indices over time are shown in Fig. 11. The total

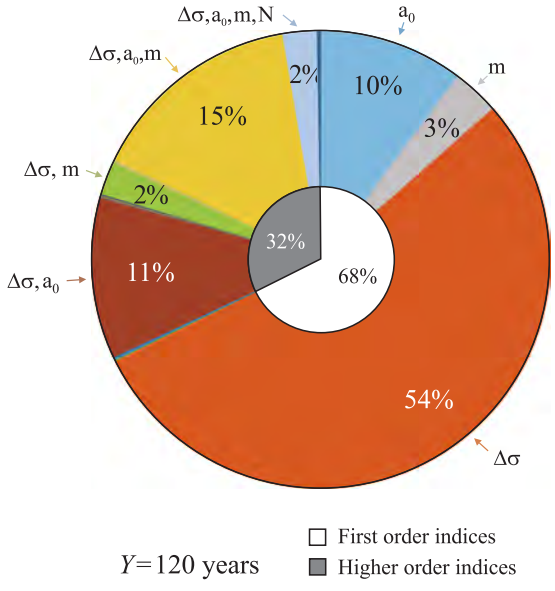

Fig. 10. First and higher-order sensitivity indices, Y = 120 years.

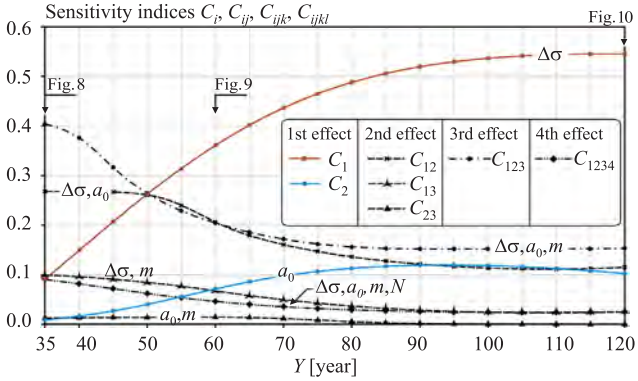

Fig. 11. First and higher-order sensitivity indices.

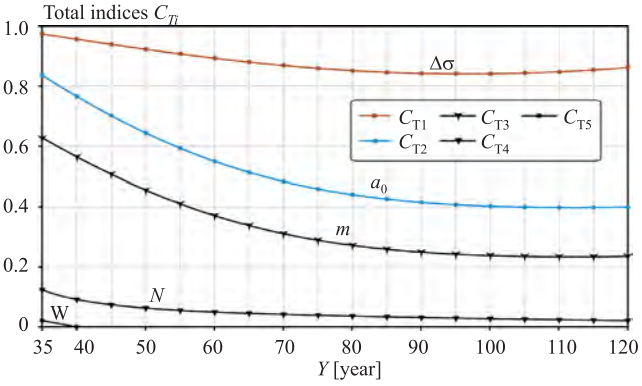

Fig. 12. Total effects on failure probability P_f.

indices C_{Ti} Eq. (10) are calculated with knowledge of all 31 indices in Eq. (8), see Fig. 12. The difference C_{Ti}-C_i is a measure of how much X_i is involved in interactions with any other variable, see Fig. 13.

5.2. PSA – observations

PSA of P_f showed that $\Delta\sigma$ is an important variable throughout the whole 120 years of operation of the bridge, see Figs. 11–13. The main effect Eq. (3) of $\Delta\sigma$ clearly increases over time (see Fig. 11), however conclusions must be made with consideration to all interaction effects.

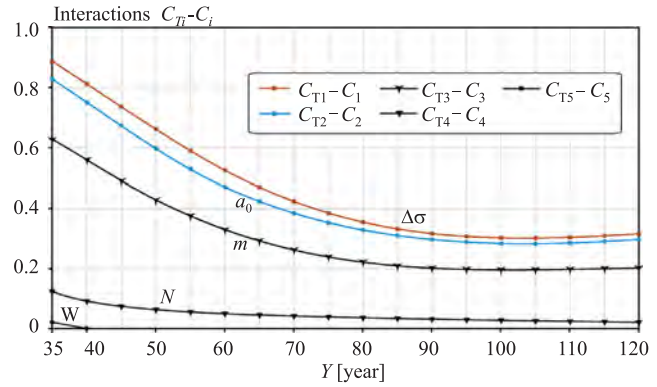

Fig. 13. Interactions effects on failure probability P_f.

While the total effect of $\Delta\sigma$ is approximately constant over time, the total effects of variables a_0 and m decrease, see Fig. 12. Thus, relative to the other variables, the total effect of $\Delta\sigma$ increases. Strong interactions are associated with small values of P_f, see Fig. 13 and Fig. 8. The interaction effects of each variable first decrease, but are approximately stable towards the end of the 120-year period, see Fig. 13. Interaction effects of $\Delta\sigma$ and a_0 are very similar (see Fig. 13), but the main effects differ (see Fig. 11).

At the end of the monitored 120-year period the sensitivity of P_f to the input variables is almost stable, both in terms of the main and the interaction effects, see Figs. 11–13. It is interesting that $\Delta\sigma$ has established itself as a more significant variable than a_0, although its variation coefficient is a third compared to a_0.

The PSA results are roughly on par with the findings of [66], where it was observed that increase in the mean stress range contributes significantly towards the decrease in the welded detail's reliability. However, the stochastic model used in [66] refers to a typical welded bridge detail and is more or less different from the model of the basic material used in this article, which mainly applies to the statistical model a_0 or the geometry function Eq. (13).

Input variables W and N were identified as completely non-influential and can be fixed anywhere in its distribution (in LHS samples) without affecting the P_f. For example, introducing random variable N or W with standard deviation of zero does not influence the results in Fig. 2. Conversely, if standard deviation equal to zero is introduced for $\Delta\sigma$, the impact on P_f and inspection times is dramatic, see Fig. 7.

Paris exponent m has a medium effect on P_f. Fixing m causes a medium change in P_f. For example, $m = 3$ will delay inspection times by approximately two years (in comparison with Fig. 2).

In this article, PSA was only performed for the zero branch, where the input random variables are mutually uncorrelated. PSA of the other branches were not performed. Therefore, the impact of input random variables on the conditional probability P_{fl} remains a question. In order to solve this task, it is necessary to develop PSA that can also take into account correlated input random variables.

PSA for $Y < 35$ years was not performed due to the extreme demands on CPU time. Reliable estimates of sensitivity indices using nested-loops require a high number of MC runs. The smaller the analysed P_f, the higher the number of MC runs needed, see for e.g. Eq. (4) and number of runs K. New computational approaches need to be developed for PSA of extremely small P_f. An approach is to substitute P_f with the reliability index β, which can be studied using quantile-oriented sensitivity analysis (QSA), where global sensitivity indices are subordinated to contrast function ψ associated with quantile [45].

Interaction effects identified by PSA and shown in Fig. 13 are relatively very high in comparison with the classic Sobol GSA, see e.g. [67,68]. Conversely, the interaction effects calculated using PSA are comparable to the interaction effects calculated using QSA [45].

6. Discussion of the results

Analysis of the probability of failure of the bridge girder (Path 0 to Path 5) identified the inspection intervals in 52.1, 62.9, 73.7, 84.6, 96.6, 109.4 years, see Fig. 2. The first inspection time $t_1 = 52.1 > 50$ theoretically exceeds 50 years of operation of the bridge, where 50 years is the medium design time for consequence Class CC2 [69]. In the case study presented here, the first inspection can be safely planned in 50 years of bridge operation and subsequent inspections with a frequency of 10 years. If a crack is detected during inspection, it is necessary to repair the bridge.

It can be noted that routine inspections of real bridges are usually planned more frequently than once every 10 years. For example, every bridge in the US is subjected to a routine inspection every two years [70]. Bridges may be exposed to greater traffic loads in combination with other negative or extraordinary influences. Cracks may develop in difficult-to-detect locations and human error in their detection cannot be ruled out.

This article deals with fatigue failures due only to traffic loads. The results of the probability and sensitivity analysis show the rationality of the presented reliability analysis, which can also be applied in other case studies. The lifetime of the bridge can practically be divided into three periods. In the first period, $P_f < P_{ft}$ and inspections are not necessary. In the second period, $P_f > P_{ft}$ and inspections and possible repairs are desired. In the third period at the end of the lifetime of the bridge, repairs can become uneconomical in ensuring sufficient reliability and the reduction of traffic load by prohibiting the passage of very heavy vehicles or closing the bridge can be discussed.

PSA identifies $\Delta\sigma$ as the dominant variable, see Fig. 12. $\Delta\sigma$ has a dominant influence on P_f and consequently on all calculated inspection times. The inspection times in Fig. 2 would shift to the left (right) if we increased (decreased) the mean value of $\Delta\sigma$ while the variation coefficient of $\Delta\sigma$ is fixed. The inspection times in Fig. 2 would shift to the left (right) if we increased (decreased) the standard deviation of $\Delta\sigma$ while the mean value of $\Delta\sigma$ is fixed. Larger standard deviation of $\Delta\sigma$ which leads to a higher probability of failure and consequently the need for earlier regular inspections. Conversely, zero standard deviation of $\Delta\sigma$ delays the first inspection by almost 18 years, see Fig. 7.

Therefore, the statistical characteristics of $\Delta\sigma$ and its pdf must be identified with maximum accuracy. The precise identification of the random variables requires prognosis of traffic load. This makes random variable $\Delta\sigma$ different from the second dominant variable a_0, whose random variability can be determined relatively accurately by experimental measurement. In general, it is advisable to identify the random variability of both $\Delta\sigma$ and a_0 as precisely as possible.

The key identifier of the influence of input variables on P_f are the total indices C_{Ti}, see Fig. 12. All decomposition indices Eq. (8) are calculated in this article with the aim of manifesting the possibilities presented by PSA. However, the calculation of all 2^M-1 sensitivity indices in Eq. (8) becomes very cumbersome or almost impossible for a higher number of input variables in Eq. (1). The PSA can escape the dimensionality curse by computing "only" M total indices Eq. (10) and M first order indices Eq. (3). The sum of all C_{Ti} is typically greater than 1. It is equal to 1 if interactions effects are absent.

Only Path 0 was studied using PSA. The other paths were studied using the screening method. Screening of random samples $\Delta\sigma$, a_0 and m shows the most important changes that occur during the exclusion of MC samples during inspection (on the target probability level P_{ft}) and identifies their impact on the calculation of the conditional probabilities. The negative correlation between $\Delta\sigma$ and a_0 resulting from the exclusion of MC samples with relatively higher random realizations of $\Delta\sigma$ and a_0 has the primary effect on the extension of inspection intervals. The introduction of $\Delta\sigma$ as non-random variables (constants) leads to perfectly regular (constant) inspection intervals (see Fig. 7), otherwise, each subsequent interval is slightly longer (see Fig. 2).

7. Conclusions

The article provides a coherent methodology of probabilistic and sensitivity analysis that can be used for decision-making on inspections, maintenance, repairs and load-bearing capacity of the bridge at different periods of its lifetime. Probabilistic and sensitivity analyses were used to examine the reliability and lifetime of a steel bridge girder subjected to fatigue failure. The presented reliability analysis takes into account fatigue failure caused by multiple repeated traffic load and disregards other negative influences.

The Bayesian interpretation of probability and linear elastic fracture mechanics were implemented in order to estimate the failure probability and propose optimal inspection times aimed at detecting fatigue damage of the bridge. Inspections are planned at the time of reaching the target failure probability of 0.02277. The case study identified inspections as periodic with a frequency of every ten years, the first inspection being carried out at fifty years of bridge operation. It was shown that inspections should be planned much earlier and should be more frequent if there is an increase in the mean value and/or standard deviation of the equivalent stress range $\Delta\sigma$ caused by the passage of heavy vehicles.

A new in-depth perspective on the influence of input random variables on the failure probability P_f over time has been provided by the application of a new type of global sensitivity analysis oriented directly at P_f, which is referred to as PSA in this article. The results obtained by PSA identify the influence of input variables on P_f changing significantly from 35 to 120 years of the bridge lifetime. PSA identified the equivalent stress range $\Delta\sigma$ as the dominant variable throughout the considered period. The probabilistic analysis confirmed that a small change in the mean value or standard deviation of $\Delta\sigma$ leads to large changes in P_f and hence to major changes in the planned inspection times. The second dominant variable is the initial edge crack length a_0. Both $\Delta\sigma$, a_0 are involved in strong interaction effects (mutually and also with the other variables) in particular on small probability of failure at the beginning of the monitored period of bridge operation (35 years). At the end of the monitored period (120 years), the dominance of $\Delta\sigma$ grows and the interaction effects of $\Delta\sigma$ with other variables decrease.

The strong influence of $\Delta\sigma$ on P_f implies that the residual lifetime of the bridge can be effectively extended by limiting very heavy vehicles, especially at the end of the bridge's lifetime. On the contrary, the sensitivity of P_f to the random variability of the specimen width W and number of load cycles N per year is very low. W and N can be fixed at any value within the range of their uncertainties without significantly influencing the P_f.

In general, the probability of failure is the basic indicator of structural reliability. The presented methodology can also be applied to other case studies, for example, with extension to weld joints, corrosion, or the analysis of structural reliability at the time of design. PSA is proving to be a useful tool in determining the influence of the uncertainty of input variables on the probability of failure. The results of PSA can change the order of importance of input variables of stochastic models aimed at probabilistic analysis. This makes PSA a very powerful tool, which deserves further development in the future. New implementation of PSA should be sought in the theory of structural reliability.

Acknowledgements

The article was elaborated within the framework of project GAČR 17-01589S.

References

[1] Kuzawa M, Kaminski T, Bien J. Fatigue assessment procedure for old riveted road bridges. Arch Civil Mech Eng 2018;18(4):1259–74.
[2] Ye XW, Su YH, Han JP. A State-of-the-art review on fatigue life assessment of steel bridges. Mathem Probl Eng 2014 2014. 13 pages.
[3] Leander J, Honfi D, Ivanov OL, Bjornsson I. A decision support framework for fatigue assessment of steel bridges. Eng Fail Anal 2018;91:306–14.
[4] Maljaars J, Bonet E, Pijpers RJM. Fatigue resistance of the deck plate in steel orthotropic deck structures. Eng Fract Mech 2018;201:214–28.
[5] Marques F, Correia JAFO, de Jesus AMP, Cunha A, Caetano E, Fernandes AA. Fatigue analysis of a railway bridge based on fracture mechanics and local modelling of riveted connections. Eng Fail Anal 2018;94:121–44.
[6] Sun B. A continuum model for damage evolution simulation of the high strength bridge wires due to corrosion fatigue. J Constr Steel Res 2018;146:76–83.
[7] Peng D, Jones R, Cairns K, Baker J, McMillan A. Life cycle analysis of steel railway bridges. Theor Appl Fract Mech 2018;97:385–99.
[8] McAllister TP, Ellingwood BR. Evaluation of crack growth in miter gate weldments using stochastic fracture mechanics. Struct Saf 2001;23(4):445–65.
[9] Tomica V, Vičan J. Effect of inspections on the existing bridges, buckling. Proceedings of the International Conference EUROSTEEL '99. ČVUT. 1999. p. 423–6.
[10] Tomica V, Krejsa M, Gocal J. Acceptable fatigue crack size – application. Trans VSB – Tech Univ Ostrava Civil Eng Series 2008;8(1):109–22.
[11] Krejsa M, Koubova L, Flodr J, Protivinsky J, Nguyen QT. Probabilistic prediction of fatigue damage based on linear fracture mechanics. Frattura ed Integrità Strutturale 2017;39:143–59.
[12] Krejsa M, Kala Z, Seitl S. Inspection based probabilistic modeling of fatigue crack progression. Procedia Eng 2016;142:146–53.
[13] Maljaars J, Vrouwenvelder ACWM. Probabilistic fatigue life updating accounting for inspections of multiple critical locations. Int J Fatigue 2014;68:24–37.
[14] Doshi K, Roy T, Parihar YS. Reliability based inspection planning using fracture mechanics based fatigue evaluations for ship structural details. Mar Struct 2017;54:1–22.
[15] Saltelli A, Tarantola S, Campolongo F, Ratto M. Sensitivity analysis in practice: a guide to assessing scientific models. New York: John Wiley and Sons; 2004.
[16] Aven T. Risk assessment and risk management: review of recent advances on their foundation. Eur J Oper Res 2016;253(1):1–13.
[17] Xiao S, Lu Z. Structural reliability sensitivity analysis based on classification of model output. Aerosp Sci Technol 2017;71:52–61.
[18] Wei P, Lu Z, Song J. Variable importance analysis: a comprehensive review. Reliab Eng Syst Saf 2015;142:399–432.
[19] Borgonovo E, Plischke E. Sensitivity analysis: a review of recent advances. Eur J Oper Res 2016;248(3):869–87.
[20] Ferretti F, Saltelli A, Tarantola S. Trends in sensitivity analysis practice in the last decade. Sci Total Environ 2016;568:666–70.
[21] Iman RL, Johnson ME, Watson Jr. CC. Sensitivity analysis for computer model projections of hurricane losses. Risk Anal 2005;25(5):1277–97.
[22] Xiao S, Lu Z, Xu L. A new effective screening design for structural sensitivity analysis of failure probability with the epistemic uncertainty. Reliab Eng Syst Saf 2016;156:1–14.
[23] Sobol' IM. Sensitivity estimates for non-linear mathematical models. Mathematical Modelling and Computational Experiment 1993;1(4):407–414. [Translated from Russian. Sobol', IM. Sensitivity estimates for nonlinear mathematical models. Matematicheskoe Modelirovanie, 1990; 2(1):112–118].
[24] Sobol' IM. Global sensitivity indices for nonlinear mathematical models and their Monte Carlo estimates. Math Comput Simul 2001;55(1–3):271–80.
[25] Yun W, Lu Z, Jiang X. An efficient method for moment-independent global sensitivity analysis by dimensional reduction technique and principle of maximum entropy. Reliab Eng Syst Saf 2018;187:174–82.
[26] Wei P, Lu Z, Song J. Regional and parametric sensitivity analysis of Sobol' indices. Reliab Eng Syst Saf 2015;137:87–100.
[27] Borgonovo E. Measuring uncertainty importance: investigation and comparison of alternative approaches. Risk Anal 2006;26(5):1349–61.
[28] Song S, Lu Z, Qiao H. Subset simulation for structural reliability sensitivity analysis. Reliab Eng Syst Saf 2009;94(2):658–65.
[29] Melchers RE, Ahammed M. A fast approximate method for parameter sensitivity estimation in Monte Carlo structural reliability. Comput Struct 2004;82(1):55–61.
[30] Ahammed M, Melchers RE. Gradient and parameter sensitivity estimation for systems evaluated using Monte Carlo analysis. Reliab Eng Syst Saf 2006;91(5):594–601.
[31] Lu Z, Song S, Yue Z, Wang J. Reliability sensitivity method by line sampling. Struct Saf 2008;30(6):517–32.
[32] Dubourg V, Sudret B. Meta-model-based importance sampling for reliability sensitivity analysis. Struct Saf 2014;49:27–36.
[33] Leander J, Al-Emrani M. Reliability-based fatigue assessment of steel bridges using LEFM – A sensitivity analysis. Int J Fatigue 2016;93:82–91.
[34] Yun W, Lu Z, Zhang L, Jiang X. An efficient global reliability sensitivity analysis algorithm based on classification of model output and subset simulation. Struct Saf 2018;74:49–57.
[35] Wang Y, Xiao S, Lu Z. An efficient method based on Bayes' theorem to estimate the failure-probability-based sensitivity measure. Mech Syst Sig Process 2019;115:607–20.
[36] Kala Z. Sensitivity and reliability analyses of lateral-torsional buckling resistance of steel beams. Arch Civil Mech Eng 2015;15(4):1098–107.
[37] Kala Z. Global sensitivity analysis in stability problems of steel frame structures. J Civil Eng Manage 2016;22(3):417–24.
[38] Kala Z, Valeš J. Sensitivity assessment and lateral-torsional buckling design of I-beams using solid finite elements. J Constr Steel Res 2017;139:110–22.
[39] Wei P, Lu Z, Hao W, Feng J. Efficient sampling methods for global reliability sensitivity analysis. Comput Phys Commun 2012;183(8):1728–43.

[40] Rahman S. A surrogate method for density-based global sensitivity analysis. Reliab Eng Syst Saf 2016;155:224–35.
[41] Yun W, Lu Z, Jiang X. A modified importance sampling method for structural reliability and its global reliability sensitivity analysis. Struct Multidiscip Optim 2018;57(4):1625–41.
[42] Fort JC, Klein T, Rachdi N. New sensitivity analysis subordinated to a contrast. Commun Statist – Theory Methods 2016;45(15):4349–64.
[43] Maume-Deschamps V, Niang I. Estimation of quantile oriented sensitivity indices. Statist Probabil Lett 2018;134:122–7.
[44] Kala Z. Benchmark of goal oriented sensitivity analysis methods using Ishigami function. Int J Mathem Comput Methods 2018;3:43–50.
[45] Kala Z. Quantile-oriented global sensitivity analysis of design resistance. J Civil Eng Manage 2019;25(4):297–305.
[46] Kala Z, Omishore A, Seitl S, Krejsa M, Kala J. The effect of skewness and kurtosis on the probability evaluation of fatigue limit states. Int J Mech 2017;11:166–75.
[47] Paris PC, Erdogan F. A critical analysis of crack propagation laws. J Basic Eng 1963;85(4):528–34.
[48] Broek D. Elementary engineering fracture mechanics. fourth ed. Dordrecht, The Netherlands: Martinus Nijhoff; 1986.
[49] Seitl S, Miarka P, Kala Z. Geometry functions for edge cracks in steel bridge under three- and four- point bending with various span. Trans VSB – Tech Univ Ostrava Civil Eng Series 2018;18(2):44–9.
[50] Seitl S, Miarka P, Malíková L, Krejsa M. Comparison of calibration functions for short edge cracks under selected loads. Key Eng Mater 2017;754:353–6.
[51] Seitl S, Miarka P, Kala Z, Klusák J. Effect of rivet holes on calibration curves for edge cracks under various loading types in steel bridge structure. Procedia Struct Integrity 2017;5:697–704.
[52] Tada H, Paris PC, Irwin GR. The stress analysis of cracks handbook. New York: ASME Press; 2000.
[53] Murakami Y. Stress intensity factors handbook. New York: Pergamon Press; 1986.
[54] Kala Z. Probabilistic modelling of fatigue crack - Some observations about conditional probability. Int J Mech 2018;12:121–30.
[55] Kala Z. Sensitivity fatigue analysis of steel structure subjected to repeated loading. Proceedings of the international on computational methods for coupled problems in science and engineering. 2005. p. 1–6.
[56] Kala Z. Fuzzy probability analysis of the fatigue resistance of steel structural members under bending. J Civil Eng Manage 2008;14(1):67–72.
[57] Maljaars J, Vrouwenvelder T. Fatigue failure analysis of stay cables with initial defects: Ewijk bridge case study. Struct Saf 2014;51:47–56.
[58] Kala Z. Stochastic inverse analysis of fatigue cracks based on linear fracture mechanics. Int J Mathem Comput Methods 2017;2:60–5.
[59] Kwon K, Frangopol DM. Bridge fatigue reliability assessment using probability density functions of equivalent stress range based on field monitoring data. Int J Fatigue 2010;32:1221–32.
[60] Downing SD, Socie DF. Simple rainflow counting algorithms. Int J Fatigue 1982;4(1):31–40.
[61] Rubinstein RY. Simulation and the Monte Carlo method. New York: John Wiley and Sons; 1981.
[62] ISO 13822. Bases for design of structures – Assessment of existing structures. Geneve, Switzerland: ISO TC98/SC2; 2010.
[63] Lesiuk G, Szata M, Bocian M. The mechanical properties and the microstructural degradation effect in an old low carbon steels after 100-years operating time. Arch Civil Mech Eng 2015;15(4):786–97.
[64] McKey MD, Conover WJ, Beckman RJ. A comparison of the three methods of selecting values of input variables in the analysis of output from a computer code. Technometrics 1979;1(2):239–45.
[65] Iman RC, Conover WJ. Small sample sensitivity analysis techniques for computer models with an application to risk assessment. Comm Statist Theory Methods 1980;9(17):1749–842.
[66] Righiniotis TD. Effects of increasing traffic loads on the fatigue reliability of a typical welded bridge detail. Int J Fatigue 2006;28(8):873–80.
[67] Kala Z, Valeš J. Global sensitivity analysis of lateral-torsional buckling resistance based on finite element simulations. Eng Struct 2017;134:37–47.
[68] Kala Z, Valeš J. Imperfection sensitivity analysis of steel columns at ultimate limit state. Arch Civil Mech Eng 2018;18(4):1207–18.
[69] EN 1990. Eurocode – Basis of structural design. Brussels: CEN; 2002.
[70] Code of Federal Regulations, National Bridge Inspection Standards – 23CFR650. U. S. Government Publishing Office, revised April 1; 2011.